Electronic Structure of Silver Oxides Investigated by Ag*L* XANES Spectroscopy

Peter Behrens[a, 1)], Stefanie Aßmann[b], Uta Bilow[c], Christoph Linke[c], Martin Jansen[c,*]

[a] München, Institut für Anorganische Chemie der Ludwig-Maximilians-Universität München
[b] Konstanz, Fakultät für Chemie der Universität
[c] Stuttgart, Max-Planck-Institut für Festkörperforschung

Received June 15th, 1998.

Abstract. The chemistry of binary and multinary silver oxides spans from subvalent species (with a mean oxidation number for Ag smaller than +1) to compounds with Ag in high oxidation states as +2 and +3. We have investigated a range of silver oxides, including the binary compounds Ag_2O, AgO, Ag_3O_4 and Ag_2O_3 as well as subvalent ternary oxides, by AgL_3 and AgL_1 XANES spectroscopy. The different valence states of silver are clearly reflected in AgL_3 and AgL_1 XANES spectra. The method thus allows the determination of average oxidation numbers. In addition, the degree of electronic interaction (localized or delocalized electronic states) in silver-oxygen compounds can be estimated on the basis of AgL_3 XANES spectra.

Keywords: Silver oxides; XANES; electronic structure; subvalent compounds

Untersuchung der elektronischen Struktur von Silberoxiden mit der Ag*L*-XANES-Spektroskopie

Inhaltsübersicht. Die Chemie binärer und multinärer Silberoxide reicht von subvalenten Spezies (mit einer mittleren Oxidationsstufe von Ag, die kleiner als +1 ist) bis zu Verbindungen mit Ag in höheren Oxidationsstufen wie +2 und +3. Wir haben eine Reihe von Silberoxiden mit der AgL_3- und der AgL_1-XANES-Spektroskopie untersucht, darunter die binären Oxide Ag_2O, AgO, Ag_3O_4 und Ag_2O_3 wie auch subvalente ternäre Oxide. Die unterschiedlichen Valenzzustände des Silbers spiegeln sich deutlich in den AgL_3- und AgL_1-XANES-Spektren wider. Diese Methode erlaubt somit die Bestimmung von mittleren Oxidationszahlen. Zusätzlich kann auch das Ausmaß der elektronischen Wechselwirkung (lokalisierte oder delokalisierte elektronische Zustände) in Silber–Sauerstoff-Verbindungen mit Hilfe von AgL_3-XANES-Spektren abgeschätzt werden.

Introduction

The electronic structure of group Ib (group 11) metal oxides is currently an active field of investigation. This is due to the interest in high-temperature superconductivity of multinary copper oxides and to special phenomena observed in crystal structures of silver oxide compounds. Ag^I oxides show a preference for linear coordination of silver and a tendency to accumulate the silver cations in common parts of the structure [1]. Of course, these peculiarities in the geometric structures must be reflected by special features in the electronic structures. The interest in silver oxides and their electronic structures also arises from the use of Ag-containing catalysts in oxidation reactions and the possible occurrence of higher oxidation states (> +1) of Ag in electrochemical processes.

X-ray absorption spectroscopy (XAS) has developed into a powerful tool for the elucidation of the geometric and electronic structures of crystalline and amorphous solids [2, 3]. The X-ray absorption near edge structure (XANES) provides direct information about the unoccupied electronic states of a material. The technique is selective with regard to the element as well as to the initial and – via the dipole selection rule – to the final state of the electronic transition [3]. It is particularly well-suited for the analysis of bond-

* Prof. Dr. M. Jansen
Max-Planck-Institut für Festkörperforschung
Heisenbergstr. 1
D-70569 Stuttgart

[1)] neue Adresse:
Institut für Anorganische Chemie
Universität Hannover
Callinstraße 9
D-30167 Hannover

  0044–2313/99/625111–116 $ 17.50+.50/0

ing in silver compounds of various oxidation states, since their electronic structures typically show small fractions of unoccupied *d* states.

A previous AgL_3 XANES study [4] has provided evidence that a small part of the formally filled $4d^{10}$ shell of the Ag^+ cations is unoccupied in oxidic compounds of Ag^I, and that this depletion of electrons in the $4d$ states is proportional to the degree of covalent bonding. In the case of silver(I) oxide Ag_2O, band structure calculations of *Czyzyk* et al. [5] (using the augmented spherical wave method) also lend support to the assumption that holes are present in the $4d$ shell of the Ag^I cations. Ag*L* XANES spectra calculated on the basis of the band structures showed acceptable agreement with the experiment. Similar results were obtained on $AgNbO_3$ [6].

In the present study, we extend the application of Ag*L* XANES spectroscopy to oxide compounds containing silver in higher and lower oxidation states. Most of the high- and sub-valent compounds investigated here have only recently become available. Their syntheses require the application of special methods. Among them are silver(II,III) oxide Ag_3O_4 [7, 8] and silver(III) oxide Ag_2O_3 [9, 10] as well as compounds containing subvalent silver, Ag_5SiO_4 [11] and Ag_5GeO_4 [12, 13]. For comparison, the well-known binary silver oxides Ag_2O and AgO [14, 15], the silver(I) silicate $Ag_{10}Si_4O_{13}$ [16], the germanate $Ag_2Ge_2O_5$ [17] as well as the silver(III) complex $Na_5[Ag(IO_5OH)_2] \cdot 11\,H_2O$ [18] have been included in the study.

Experimental

Samples

Binary silver oxides containing silver in oxidation states higher than +1 were prepared by anodic oxidation of aqueous solutions of silver salts like $AgClO_4$ or $AgPF_6$ [7–10, 19] on a platinum wire electrode (surface area: 130 mm^2). In detail, AgO was prepared by electrolysis of a solution containing 0.03 mol/L Ag^+ and 0.3 mol/L F^- (from the addition of NaF) at 95 °C. The solution was placed in a 100 mL Teflon beaker; a Pt net served as counter electrode. The applied current started at 3 mA, increased to 10 mA within 100 minutes, was fixed at this value for 70 minutes and finally lowered to 7 mA within 45 minutes. For Ag_3O_4, the initial solution contained 0.1 mol/L Ag^+ and 2.0 mol/L F^-. The solution was cooled to 0 °C and filled into a 100 mL Pt crucible which also served as a counter electrode. Constant current electrolysis was carried out at 12 mA for 2 h. Ag_2O_3 is obtained from a 0.1 mol/L solution of $AgBF_4$ at 0 °C. Using a Pt net as a counter electrode, constant current electrolysis was carried out at 20 mA for 2 h. In all cases, the crystals harvested from the Pt wire were washed with ice-cold water and dried at reduced pressure in an oxygen stream at a temperature of 0 °C. Because of their tendency to loose oxygen, the compounds were stored below –25 °C.

Compounds containing subvalent silver were prepared according to published procedures [11–13].

Ag_2O was purchased (Merck 1503). Other compounds were prepared as described in the literature ($Ag_{10}Si_4O_{13}$ [16]; $Ag_2Ge_2O_5$ [17]; $Na_5[Ag(IO_5OH)_2] \cdot 11\,H_2O$ [18]). All samples were checked for phase purity by powder X-ray diffraction. A silver foil from Goodfellow was used as a sample of elemental silver.

X-ray absorption spectroscopy

For XAS measurements carefully ground powders of the substances (except for the Ag foil) were pressed to polyethylene pellets (spectroscopic grade polyethylene: Merck 7422). The amount of sample was adjusted to give edge jumps $\Delta\mu d$ of about 0.5 at the AgL_3 edge. This small value was chosen in order to avoid thickness effects. Samples containing high-valent silver were cooled during this procedure.

Ag*L* edge X-ray absorption spectra were collected at the EXAFS-II station [20] at HASYLAB/Hamburg/Germany using synchrotron radiation from the storage ring DORIS II operated at 5.301 GeV with currents between 40 and 20 mA during parasitic beam-time. The spectrometer was equipped with a focussing mirror covered with a Ni alloy and a Si(111) double crystal monochromator. The reflectivity cut-off of the mirror at about 7 keV and a detuning of the monochromator to about 50% of the maximum intensity effectively served to reduce contributions from higher energy harmonics to the X-ray beam. Absorption spectra were obtained in the transmission mode using ionization chambers to determine the intensities of the X-ray beam both in front of and behind the sample. During the measurements, samples were placed *in vacuo* in order to avoid absorption of the soft X-rays used. The compounds containing silver of higher valency were cooled by means of a liquid helium cryostat while evacuating the sample chamber in order to prevent them from loosing oxygen. Spectra for these samples were measured at 40 K. All other spectra were recorded with the sample at room temperature.

AgL_3 and AgL_1 edge regions were scanned with a stepwidth of 0.25 eV, well below the estimated experimental resolution of ca. 0.6 eV. For calibration of the energy *E*, a Pd metal foil was scanned simultaneously with each sample, using the count rates of the second and a third ionization chamber. The energy scale of AgL_3 spectra was fixed by setting the inflection point of the rising PdL_2 edge to $E = 3.3303$ keV, giving a relative calibration error < 0.2 eV between different scans. AgL_1 edges were calibrated against the PdL_1 edge of elemental Pd. The L_1 edge energy of 3607 keV was ascribed to the inflection point of the rising PdL_1 edge. High-quality L_3 spectra were obtained for both the silver-containing sample and the Pd foil. The quality of the L_1 spectra suffered from the small edge jump (typically 1/4 of that at the L_3 edge) and the high background absorption of the preceding L_3 and L_2 edges. Whereas AgL_1 spectra of reasonable quality could still be obtained, the PdL_1 data often were noisy. Therefore, the estimated relative calibration error of AgL_1 XANES spectra is about ±0.5 eV.

For the analysis, usual data reduction procedures were followed, applying a Victoreen-type fit for the slow decay of the absorption before the edge and normalization of the amplitude of the spectra to an absorption $\mu d = 1$ at an energy about 100 eV above the edge. Further data evaluation is described in the following section.

Results

AgL_3 XANES

AgL_3 spectra of the samples investigated are shown in Figure 1 (in all Figures, the compound $Na_5[Ag(IO_5OH)_2] \cdot 11\,H_2O$ is denoted as "Ag(III) complex"). All spectra except for that of elemental Ag show an absorption at about 3.35 keV (denoted **A**) which is attributed to dipole-allowed $2p_{3/2} \rightarrow 4\,d$ transitions [4, 5]. In order to evaluate the intensity of this feature, the spectra of all compounds were deconvoluted using a least-squares-minimization procedure with a Lorentzian line shape for the absorption at about 3.35 keV, a modified arctangent function for the rise of the edge and asymmetric Gaussian peaks to model additional humps present in the spectra. Typical fits are shown in Figure 2. Table 1 lists the intensities of these peaks defined as $I(\mathbf{A}) = height \times HWHM$ (*HWHM*: half width at half maximum in eV). Several fit models involving different peak functions and varying positions of the edge (which, however, was always kept above 3.36 keV) were tried. Although the absolute values of $I(\mathbf{A})$ varied with the edge position, their ratios were not significantly influenced (note that the fit model chosen here differs slightly from that used in [4], so that the absolute values for $I(\mathbf{A})$ of Ag_2O and of the Ag(III) complex given here are slightly different from those given there). For the subvalent Ag oxide compounds,

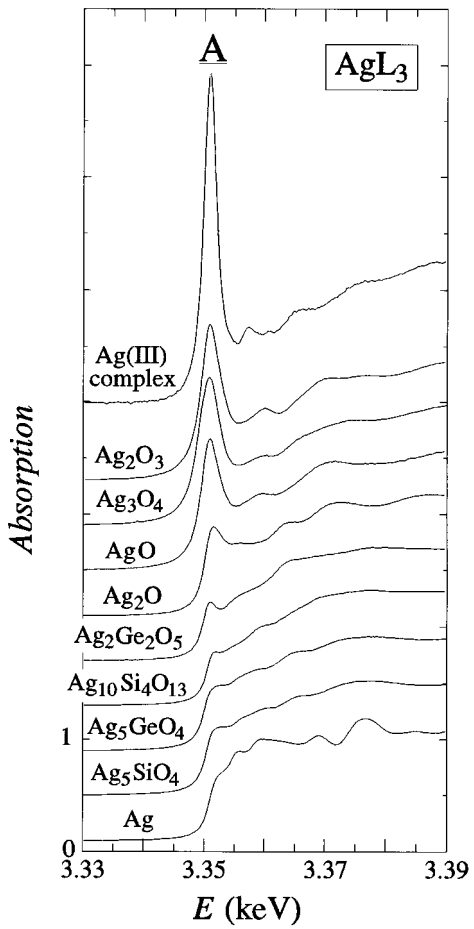

Fig. 1 AgL_3 XANES spectra of elemental Ag and various silver oxide compounds.

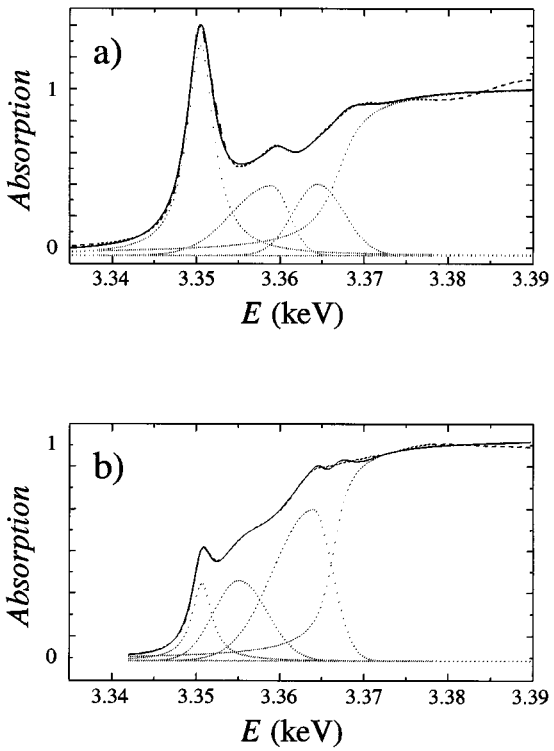

Fig. 2 Typical results of fits to the AgL_3 XANES: a) Ag_2O_3, b) $Ag_2Ge_2O_5$. Broken line: experimental data; full line: fit; dotted lines: single fit functions (a Lorentzian for peak **A** at about 3.351 keV, asymmetric Gaussians for additional humps, a modified arctangent function for the rise of the edge and a constant with a small negative value).

Table 1 Intensities $I(\mathbf{A})$ (in arbitrary units) of AgL_3 XANES peaks **A** at about 3.35 keV resulting from the fit procedure and positions of the AgL_1 edge $E(\mathbf{B})$ as determined from the second derivative of the absorption *vs.* energy. Oxidation states of the compounds are also given

sample	oxidation states	average oxidation number	$I(\mathbf{A})$	$E(\mathbf{B})$ (keV)
$Na_5[Ag(IO_5OH)_2] \cdot 11\,H_2O$	+III	+3	5.3(2)	3.8155(5)
Ag_2O_3	+III	+3	4.7(2)	3.8153(5)
Ag_3O_4	+II, +III	+2.67	4.9(2)	3.8139(5)
AgO	+I, +III	+2	3.6(2)	3.8108(5)
Ag_2O	+I	+1	1.7(1)	3.8096(5)
$Ag_2Ge_2O_5$	+I	+1	1.0(2)	3.8101(5)
$Ag_{10}Si_4O_{13}$	+I	+1	0.9(2)	3.8105(5)
Ag_5GeO_4	+I, +1 e^-	+0.8	1.1(3)	3.8092(5)
Ag_5SiO_4	+I, +1 e^-	+0.8	1.2(3)	3.8090(5)
Ag	0	0	–	3.8065(5)

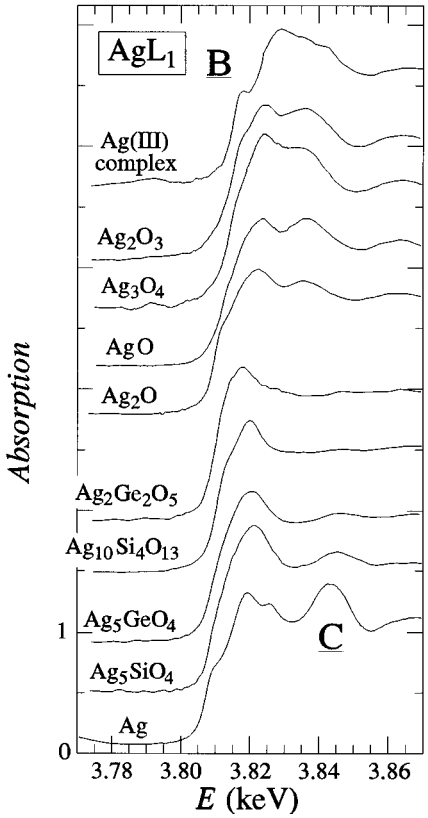

Fig. 3 AgL_1 XANES spectra of elemental Ag and various silver oxide compounds.

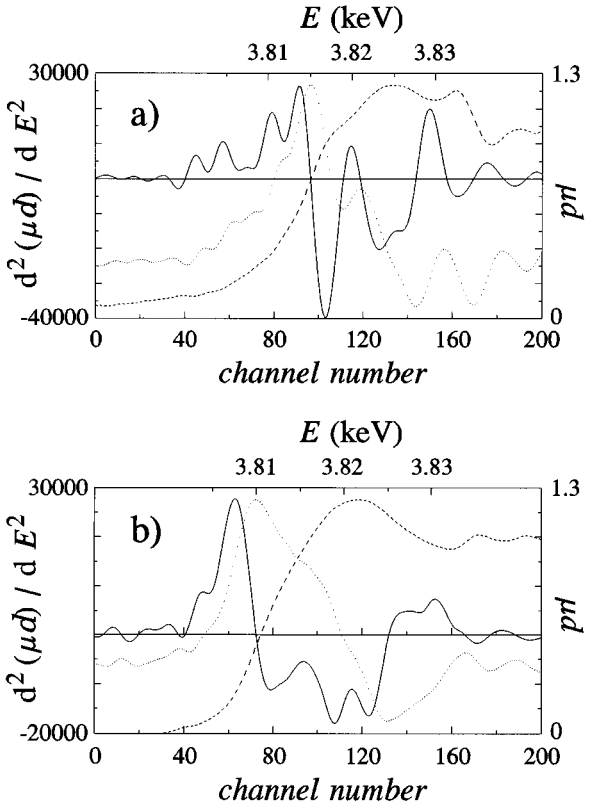

Fig. 4 Determination of the edge position E(**B**) of AgL_1 XANES spectra: a) Ag_2O_3, b) $Ag_2Ge_2O_5$. E(**B**) is taken as the zero value of the second derivative $d^2(\mu d)/dE^2$ corresponding to the inflection point of $\mu d(E)$. Broken line: $\mu d(E)$; dotted line: $d(\mu d)/dE$; full line: $d^2(\mu d)/dE^2$.

the given I(**A**) values are afflicted with larger errors, because the corresponding absorptions appear only as shoulders, but not as distinct peaks. For Ag metal, no peak **A** was observed.

AgL_1 XANES

AgL_1 XANES spectra are shown in Figure 3. The oscillations in the pre-edge background stem from the fading AgL_2 EXAFS. They vary only little with E and should therefore not influence the evaluation of AgL_1 XANES data significantly. As shown for two examples in Figure 4, the edge position E(**B**) was determined by the point where the second derivative $d^2(\mu d)/dE^2$, corresponding to the inflection point of $\mu d(E)$, vanishes. E(**B**) values are given in Table 1 and Figure 5 shows a plot of E(**B**) *vs.* the average oxidation number of Ag in the compounds.

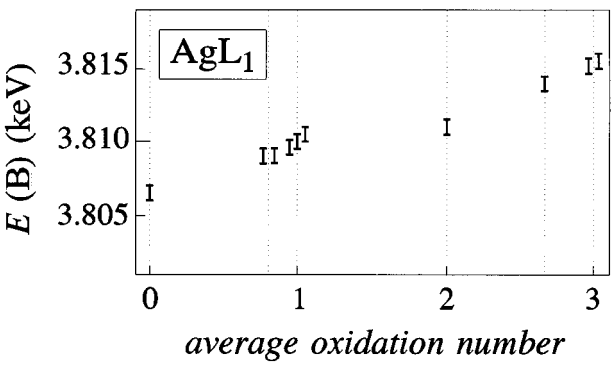

Fig. 5 Edge position E(**B**) of AgL_1 XANES spectra *vs.* the average oxidation number of silver-oxygen compounds.

Discussion

AgL_3 XANES

The most remarkable feature of the AgL_3 XANES spectra is the absorption **A** at about 3.35 keV. From previous experimental [4, 5] and theoretical [5] investigations it can be ascribed unambigously to a dipole-allowed $2p_{3/2} \rightarrow 4d$ transition. Its intensity is directly related to the de-occupation of states derived from Ag $4d$ orbitals. Correspondingly, I(**A**) increases with the average oxidation number. The following points are worth mentioning:

– Feature **A** is absent for elemental Ag, *i. e.* in elemental Ag all Ag $4d$ states are occupied.

– Feature **A** is present in the Ag(I) oxide compounds. Its intensity is small for the compounds where ionic bonding prevails ($Ag_{10}Si_4O_{13}$, $Ag_2Ge_2O_5$) and stronger for compounds bonded mostly covalently, like Ag_2O. This is in line with former observations [4]: In Ag(I) oxides the Ag $4d$ states are partly depleted in spite of the rule that filled sub-shells (like the formal $4d^{10}$ configuration of Ag^+) do not participate in chemical bonding. The degree of depletion and thus the intensity $I(\mathbf{A})$ increases with the degree of covalent bonding. This can be explained by the consideration that covalent bonds need highly directional orbitals, as they can be created, for example, by hybridization. In the case of Ag(I) compounds, hybridization obviously includes also $4d$ orbitals and thus the formally closed sub-shell configuration $4d^{10}$ is opened. For example, in Ag_2O and other oxidic compounds as $AgCoO_2$ and $AgPbO_2$ [21], the linear coordination of the Ag^+ cations can be rationalized by assuming hybridization of Ag $4d_{z^2}$ and $5s$ orbitals [22], leading to a valence electron distribution that can be described as $4d^{10-\delta}5s^{\delta}$ (this approach can be extended to incorporate interactions with the $5p_z$ orbital in addition) [23]. When this type of hybridization occurs, the depletion of $4d$ states of Ag^I cations is strongest. The relation between peak intensity $I(\mathbf{A})$ and covalency permits the estimation of the bond character in other silver compounds, also in amorphous ones [4]. Allowing the closed-shell configuration d^{10} to interact in chemical bonding could also provide the basis for an explanation for the observed accumulation tendency of the (formally) positively charged Ag^+ ions [1].

– Based on structural considerations, the electron distribution of the semi-conducting subvalent silver oxides Ag_5EO_4 (E: Si, Ge) can be formulated as $(Ag^+)_4\,(Ag_6)^{4+}\,(EO_4^{4-})_2$ [11–13]. The following discussion relates to Ag_5SiO_4 [11], but similar arguments are valid for Ag_5GeO_4 [12, 13]. In Ag_5SiO_4, the $(Ag_6)^{4+}$ cluster forms a slightly distorted octahedron with Ag–Ag distances d_{Ag-Ag} ranging from 2.70 to 2.86 Å (in elemental silver, $d_{Ag-Ag} = 2.89$ Å). From the diamagnetic and semiconducting properties of Ag_5SiO_4, it follows that the additional electrons of this subvalent compound (one e^- per formula unit Ag_5SiO_4, two e^- per $(Ag_6)^{4+}$ cluster) are localized. It is assumed that these extra electrons occupy the skeleton orbital of lowest energy within the Ag_6 cluster. Correspondingly, the low-lying $4d$ states of the Ag atoms in the octahedral cluster should be occupied and should not contribute to the intensity of peak **A**. The isolated Ag^+ cations in the formula $(Ag^+)_4\,(Ag_6)^{4+}\,(SiO_4^{4-})_2$ exhibit larger Ag–Ag distances (d_{Ag-Ag}: 2.97 to 3.30 Å). Their coordination by oxygen is characterized by coordination numbers of 3 and atomic distances d_{Ag-O} between 2.31 and 2.34 Å, indicating partly ionic, partly covalent bonding. Due to the shape of signal **A** in the AgL_3 XANES spectra of Ag_5SiO_4 (and of Ag_5GeO_4), which does not peak but appears only as a shoulder, it was difficult to describe this feature in the fitting procedure. Within the enlarged error range, its intensity is similar to the values observed for Ag^I compounds (Table 1). This is in line with the estimate that the intensity is the sum of the individual absorptions of 3/5 Ag^+ ions with occupied $4d$ states and of 2/5 Ag^+ ions which are in a mixed bonding situation.

– For the binary silver oxides, $I(\mathbf{A})$ grows strongly with increasing average oxidation number. The increasing depletion of the Ag $4d$ states can thus directly be observed and supports the assignment of oxidation numbers larger than +1. The difference between Ag_3O_4 and Ag_2O_3 (average oxidation numbers of 2.67 and 3, resp.), however, is not reflected in the values of $I(\mathbf{A})$. This might point to special characteristics of the electronic structure of Ag_3O_4. The structural study revealed that all Ag cations possess similar coordination by oxygen, so that it was not possible to assign Ag^{II} and Ag^{III} to specific Ag sites. Thus, it was assumed that the positive charge is largely delocalized and equilibrated between all Ag sites [7, 8]. Note that $I(\mathbf{A})$ of AgO (3.6) is close to the average of the $I(\mathbf{A})$ values of Ag_2O and Ag_2O_3 (3.2), reflecting the mixed valence nature of this oxide as an $Ag^{I,III}$ oxide $Ag^+Ag^{3+}O_2$ [14, 15].

– An interesting difference is observed between the features **A** of the Ag^{III} complex compound $Na_5[Ag(IO_5OH)_2]\cdot 11\,H_2O$ and Ag_2O_3, both containing exclusively Ag^{III}. Although the intensities $I(\mathbf{A})$ are similar, signal **A** peaks at a larger absorption value in the case of the complex than in the case of the binary oxide. This is of course due to the different widths of these peaks. These widths are directly related to the widths or energy dispersions of the corresponding final states of the electronic transitions and can be rationalized as follows: In both Ag^{III} compounds, the silver ions possess a d^8 electron configuration and, as typical of this configuration, a square-planar coordination of Ag by O. In the complex, the final state of the electronic transition is the lowest unoccupied molecular orbital, namely the $4d_{x^2-y^2}$ orbital. It interacts only with symmetry-related ligand orbitals of the surrounding oxygen atoms and is highly localized. In contrast, Ag_2O_3 (isotypic with Au_2O_3) exhibits a three-dimensional framework structure [10] where extended overlap of Ag $4d$ and O $2p$ orbitals is possible. This leads to a dispersion of the electronic states derived from these orbitals, *i. e.* to a band. The black colour and the metallic lustre of Ag_2O_3 crystals support this interpretation [9]. The different widths of the unoccupied electronic states of the localized and of the band type are reflected in the widths of the $2p_{3/2} \rightarrow 4d$ transition.

AgL_1 XANES

The interpretation of the AgL_1 spectra suffers from their inferior quality as compared to the AgL_3 spectra.

– As a general trend, it can be stated that the edge position $E(\mathbf{B})$ (Table 1) shifts to higher energies with higher oxidation numbers (Figure 5), but due to uncertainties in the energy calibration of the L_1 edges (see Experimental) this relation is afflicted with rather large errors. Similar relations have been established for many other K and L_1 edges. They are generally interpreted as an increase in ionization energy with increasing positive charge on the atom (in this context, the ionization energy is the energy necessary to transfer electrons from electronic core states as $1s$ or $2s$ to the vacuum level). The relation between $E(\mathbf{B})$ and the average oxidation number gives additional support to the assignment of oxidation numbers larger than +1 in silver oxides and to the existence of subvalent silver oxide compounds. The fact that the $E(\mathbf{B})$ value for AgO appears to be too small is of course due to the fact that the first inflection point of this edge is determined by the Ag^{I} component of this $Ag^{I,III}$ oxide.

– The common appearance of a feature **C** (at E = 3.84 keV, *cf.* Fig. 3) in elemental Ag and in the subvalent silver compounds Ag_5SiO_4 and Ag_5GeO_4 is remarkable. Features in this region of XANES spectra can be explained by two different approaches, namely by multiple scattering or by the structure of the unoccupied density of states [3]. From the point of view of geometric structure, both elemental Ag and the subvalent compounds [11–13] contain a similar building unit, namely Ag_6 octahedra. In the language of multiple scattering, absorption **C** could be caused by multiple scattering pathways within these Ag_6 octahedra. From the standpoint of band theory, the unoccupied DOS of elemental Ag and of the subvalent compounds possess some similarity at about 40 eV above the vacuum level. The $(Ag_6)^{4+}$ clusters could thus be viewed as tiny pieces of silver metal, isolated from each other by the ionic $[Ag_4(EO_4)_2]^{4-}$ framework (compare the situation of rhombohedral α-boron where electron-deficient, "metallic-like" B_{12} icosahedra are electronically isolated from each other by covalent B–B bonds).

Conclusions

Our results show that the occurrence of oxidation states larger than +1 and of subvalency in silver oxide compounds is clearly reflected in AgL_3 and AgL_1 XANES spectra. The method allows the determination of average oxidation numbers. Also, the degree of electronic interaction (localized – delocalized) in silver-oxygen compounds can be classified on the basis of the width of the $2p_{3/2} \rightarrow 4d$ transition in AgL_3 XANES spectra. The possibility to perform such assignments is of special interest for non-crystalline solids (*e. g.* catalysts with non-uniform Ag distribution or layers formed on electrodes during electrochemical processes) where oxidation states cannot be assigned on the basis of detailed structural information or other physical data.

We thank the HASYLAB for allocating beam time and the HASYLAB team for excellent working conditions. The help from *Dr. Michael Fröba* during the measurements is acknowledged. This research was supported by the Deutsche Forschungsgemeinschaft and the Fonds der Chemischen Industrie.

References

[1] M. Jansen, *Angew. Chem.* **1987**, *99*, 1136; *Angew. Chem. Int. Ed. Engl.* **1987**, *26*, 1098.
[2] P. Behrens, *Trends Anal. Chem.* **1992**, *11*, 218.
[3] P. Behrens, *Trends Anal. Chem.* **1992**, *11*, 237.
[4] P. Behrens, *Solid State Commun.* **1992**, *81*, 235.
[5] M. T. Czyzyk, R. A. de Groot, G. Dalba, P. Fornasini, A. Kisiel, F. Rocca, E. Burattini, *Phys. Rev. B* **1989**, *39*, 9831.
[6] A. A. Ivantsov, A. V. Soldatov, Yu. V. Sukhetskii, A. N. Gusatinskii, A. P. Kovtun, *Phys. Status Solidi B* **1991**, *164*, K23.
[7] B. Standke, M. Jansen, Angew. Chem. **1986**, *98*, 78; *Angew. Chem. Int. Ed. Engl.* **1986**, *25*, 77.
[8] B. Standke, M. Jansen, *J. Solid State Chem.* **1987**, *67*, 278.
[9] B. Standke, M. Jansen, *Angew. Chem.* **1985**, *97*, 114; *Angew. Chem. Int. Ed. Engl.* **1985**, *24*, 118.
[10] B. Standke, M. Jansen, *Z. Anorg. Allg. Chem.* **1986**, *535*, 39.
[11] C. Linke, M. Jansen, *Inorg. Chem.* **1994**, *33*, 2614.
[12] M. Jansen, C. Linke, *Angew. Chem.* **1992**, *104*, 618; *Angew. Chem. Int. Ed. Engl.* **1992**, *31*, 653.
[13] M. Jansen, C. Linke, *Z. Anorg. Allg. Chem.* **1992**, *616*, 95.
[14] V. Scatturin, P. L. Bellon, A. J. Salkind, *J. Electrochem. Soc.* **1961**, *108*, 819.
[15] M. Jansen, P. Fischer, *J. Less-Common Met.* **1988**, *137*, 123.
[16] M. Jansen, H. L. Keller, *Angew. Chem.* **1979**, *91*, 500; *Angew. Chem Int. Ed. Engl.* **1979**, *18*, 464.
[17] M. Jansen, B. Standke, *Z. Anorg. Allg. Chem.* **1984**, *510*, 143.
[18] A. Balikungeri, M. Pelletier, D. Monnier, *Inorg. Chim. Acta* **1977**, *22*, 7.
[19] P. Fischer, M. Jansen, *Solid State Ionics* **1990**, *43*, 61.
[20] W. Malzfeldt, W. Niemann, R. Haensel, P. Rabe, *Nucl. Instrum. Meth.* **1985**, *208*, 359.
[21] P. Behrens, unpublished results.
[22] L. E. Orgel, *J. Chem. Soc.* **1958**, 4186.
[23] F. A. Cotton, G. Wilkinson, *Anorganische Chemie*, 4th ed., Verlag Chemie, Weinheim 1982, p. 985 f.